frontiers in Materials

ORIGINAL RESEARCH
published: 24 December 2021
doi: 10.3389/fmats.2021.800820

Air-Flow Impacting: A New Mechanochemical Method for Continuous, Highly Efficient, Large-Scale Synthesis of Metal–Organic Frameworks and Mechanistic Research

Jun Zhao[1,2]*

[1]State Key Laboratory of Environment-friendly Energy Materials, Southwest University of Science and Technology, Mianyang, China, [2]Sichuan College of Architecture and Technology, Deyang, China

The novel air-flow impacting (AFI) synthesis technology for mechanochemical synthesis of MOFs (ZIF-67) was first reported. AFI was an improvement of the traditional mechanochemical synthesis method. The results indicated that ZIF-67 was successfully synthesized after 30 min at a rate of 60 kg h^{-1}. The as-prepared ZIF-67 was characterized by Fourier transform infrared spectroscopy (FT-IR), powder x-ray diffraction (P-XRD), thermogravimetric analysis (DTA/TG), scanning electron microscope (SEM), transmission electron microscope (TEM), and single-crystal x-ray diffraction. The kinetic analysis of the reaction mechanism was carried out by detecting the P-XRD patterns of the products with different reaction times. The synthesis belonged to the one-dimensional diffusion-controlled model.

Keywords: air-flow impacting, metal–organic frameworks, solid-phase synthesis, ZIF-67 crystal, preparation mechanism

OPEN ACCESS

Edited by:
John L. Provis, The University of Sheffield, United Kingdom

Reviewed by:
Ratiram Gomaji Chaudhary, Seth Kesarimal Porwal College, India
Yusuf Valentino Kaneti, National Institute for Materials Science, Japan

***Correspondence:**
Jun Zhao
17683146919@163.com

Specialty section:
This article was submitted to Structural Materials, a section of the journal Frontiers in Materials

Received: *24 October 2021*
Accepted: *06 December 2021*
Published: *24 December 2021*

Citation:
Zhao J (2021) Air-Flow Impacting: A New Mechanochemical Method for Continuous, Highly Efficient, Large-Scale Synthesis of Metal–Organic Frameworks and Mechanistic Research. Front. Mater. 8:800820. doi: 10.3389/fmats.2021.800820

INTRODUCTION

ZIF-67 is a typical kind of metal–organic frame (MOF). Because of its porous and large specific surface area, it is widely used in gas storage, energy, catalysis, and chemical sensor, etc. (Wang et al., 2018; Zheng et al., 2018; Zhou et al., 2018).

MOFs are composed of metal ions and organic chains through coordination bonds, exhibiting high specific surface area, vacant coordination sites, and strong surface dipole moments, which have been widely used in the field of energy storage and conversion. Therefore, developing advanced electrocatalysts with low cost and high performance is an urgent task. Numerous efforts have been made to develop efficient non-precious metal electrocatalysts, such as metal–organic frameworks (MOFs), transition metal oxides/sulfides/selenides/phosphides, and carbon-doping semiconductor materials. Before mechanochemical synthesis (James et al., 2012; Stock and Biswas, 2012; Baláž et al., 2013; Takacs, 2013; Wang, 2013; Crawford et al., 2015), ZIF-67 was prepared through the conventional hydrothermal/solvothermal method (Panda et al., 2017). However, this traditional method required the extensive use of hostile organic solvents, thereby increasing the environmental burden. Nowadays, mechanical ball milling and twin-screw extrusion have also achieved ZIFs (Bennett et al., 2013; Crawford and Casaban, 2016). However, these synthesis techniques had many

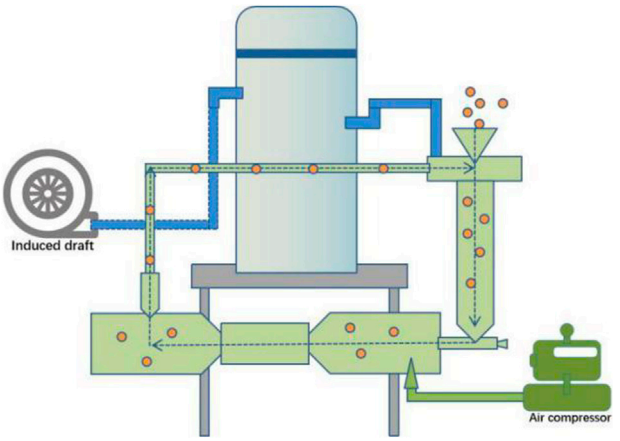

FIGURE 1 | AFI reaction equipment with key parts highlighted.

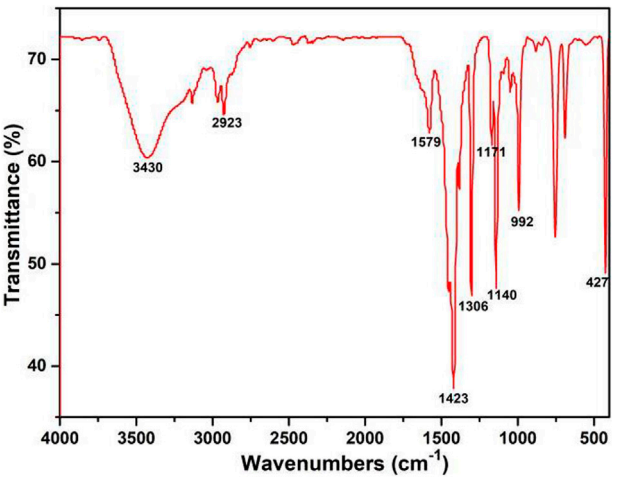

FIGURE 2 | FT-IR spectra of ZIF-67.

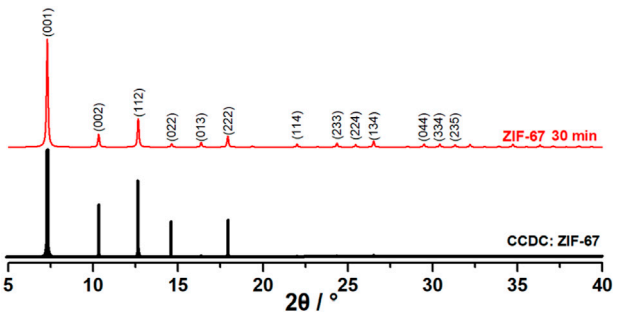

FIGURE 3 | P-XRD patterns of ZIF-67.

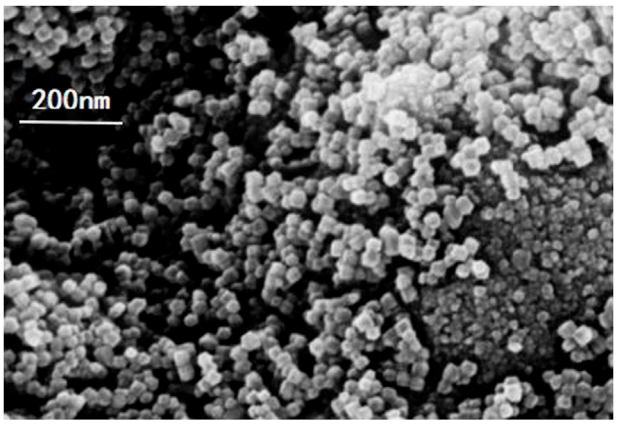

FIGURE 4 | SEM images of ZIF-67.

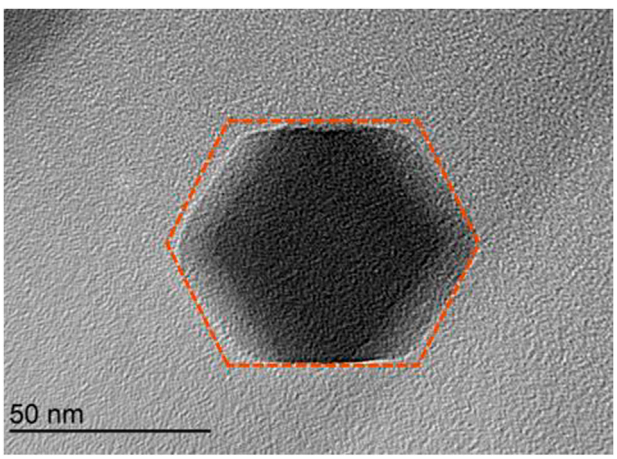

FIGURE 5 | TEM images of ZIF-67.

TABLE 1 | Crystal data and structure refinement for ZIF-67.

CCDC	1945392
Formula	$C_8H_{10}CoN_4$
M/g·mol^{-1}	221.13
T/K	293 (2)
Crystal system	Cubic
Space group	I-43 m
a/Å	17.1238(4)
b/Å	17.1238(4)
c/Å	17.1238(4)
α/°	90
β/°	90
γ/°	90
Volume/Å^3	5021.1(4)
Z	12
ρ_{calc}g/cm^3	0.878
Crystal size/mm^3	0.13 × 0.12 × 0.11
Reflections collected	3,465
Final R indexes [I>=2σ (I)]	R_1 = 0.0312, wR_2 = 0.0980
Final R indexes [all data]	R_1 = 0.0337, wR_2 = 0.0994
Refinement	SHELXL-97

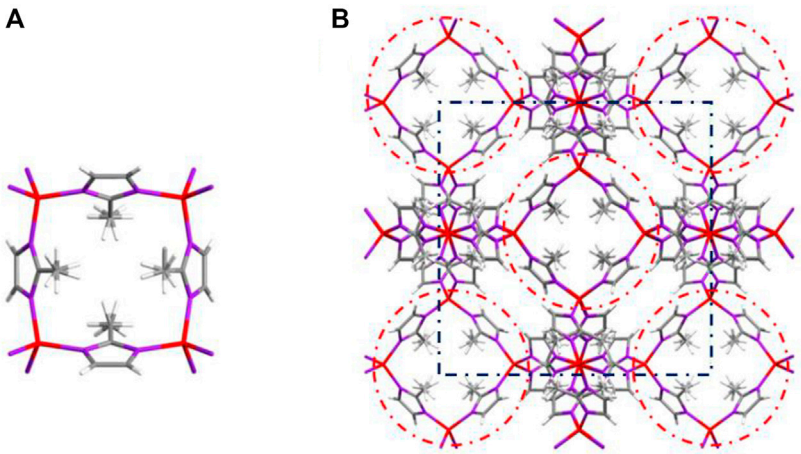

FIGURE 6 | (A) Unit lattice of ZIF-67; **(B)** crystal structure of ZIF-67.

TABLE 2 | Bond lengths for ZIF-67.

Atom	Atom	Length/Å	Atom	Atom	Length/Å
Co1	N1[a]	1.984(4)	C1	N1	1.384(7)
Co1	N1[b]	1.984(4)	C2	C3	1.465(11)
Co1	N1	1.984(4)	C2	N1	1.354(6)
Co1	N1[c]	1.984(4)	C2	N1[d]	1.354(6)

Symmetry transformation for generating equivalent atoms.
[a]*–1/2 + Z, 1/2–Y, 1/2–X.*
[b]*1/2-Z, 1/2–Y, 1/2 + X.*
[c]*–X, +Y, 1–Z.*
[d]*+X, +Z, +Y.*

TABLE 3 | Bond angles for ZIF-67.

Atom	Atom	Atom	Angle/°	Atom	Atom	Atom	Angle/°
N1[a]	Co1	N1[b]	108.87(13)	N1[d]	C2	C3	123.2(3)
N1[b]	Co1	N1	110.7(3)	N1	C2	C3	123.2(3)
N1[a]	Co1	N1	108.87(13)	N1[d]	C2	N1	113.4(7)
N1[a]	Co1	N1[c]	110.7(3)	C1	N1	Co1	126.1(4)
N1[d]	Co1	N1	108.87(13)	C2	N1	Co1	129.5(4)
N1[b]	Co1	N1[c]	108.87(13)	C2	N1	C1	104.4(5)

Symmetry transformation for generating equivalent atoms.
[a]*–1/2 + Z, 1/2-Y, 1/2-X.*
[b]*1/2-Z, 1/2-Y, 1/2 + X.*
[c]*–X, +Y, 1-Z.*
[d]*+ X, +Z, +Y.*

disadvantages. For example, mechanical ball milling could not achieve continuous production and also might pollute the products by abrasion of grinding balls as contaminants. Therefore, it was necessary to develop new mechanochemical synthesis technology.

In AFI, high-velocity airflow was introduced, and particle impact was target driven by high-speed airflow. The speed of the particle might reach up to 300 m s^{-1} or even faster (Sun et al., 2016). In addition, it is an environmentally friendly solvent-free chemical process and could achieve products in the submicron size powder form (Qian et al., 2012).

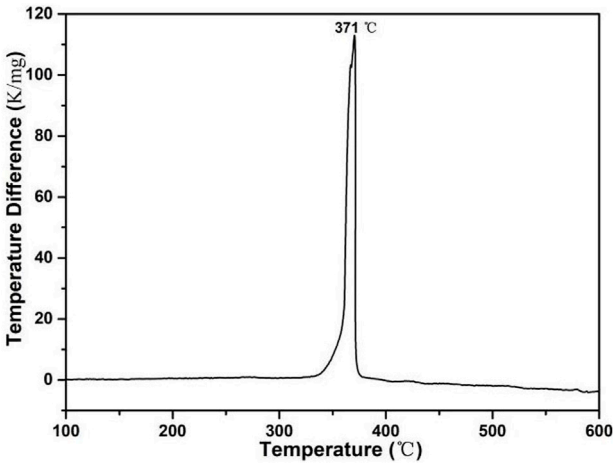

FIGURE 7 | DTA curve of ZIF-67.

EXPERIMENTAL

Chemicals and Materials

The air-flow impacting equipment is shown in **Figure 1**. First, the particles were transferred into the impacting chamber through the feed port. Then, the particles were accelerated to high velocities (300 m/s) by compressed air (1.5 MPa). In this process, there was a violent collision between reactant particles, which led to the pulverization of reactant particles and the formation of chemical reaction products. Finally, the products were collected by the circulation

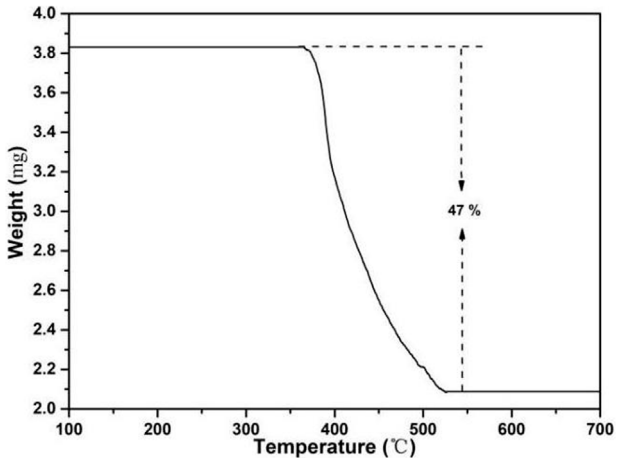

FIGURE 8 | TG curve of ZIF-67.

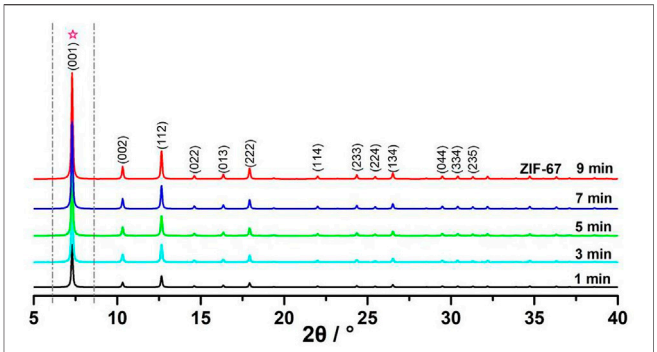

FIGURE 9 | P-XRD curves of ZIF-67 at different reaction time.

collecting system. Cobaltous oxide (CoO, 99%), 2-methylimidazole (99.99%), and potassium bisulfate (99%) were obtained from Aladdin (Shanghai, China). All reagents are of analytical grade and used without further purification.

Preparation of ZIF-67

ZIF-67 was prepared as follows: CoO (74.93 g, 1 mol), 2-methylimidazole (82.1 g, 1 mol), and potassium bisulfate (136.17 g, 1 mol) were mixed in a 1:1:1 molar ratio, and the material was placed in a 1,000-ml beaker and mixed well. Then, it was aged for 72 h in a closed environment at 30°C, and the mixture was transferred into the impacting chamber, at the rate of 1.5 kg min^{-1}. Then, compressed air (1.5 MPa) was used to accelerate the material to a supersonic speed. The purple powders were collected every 2 min until the reaction lasted for 30 min. After washing with ethanol three times, it was dried in an oven at 50°C. Yields: 87% based on 2-methylimidazole.

RESULTS AND DISCUSSION

Characterization

As shown in **Figure 2**, the FT-IR spectra of ZIF-67 synthesized by AFI was identical to previously reported studies (Qin et al., 2017). The absorption at 427 cm^{-1} was Co-N stretching vibration peak, and two peaks which were at 2,923 cm^{-1} and 1,579 cm^{-1} attributed to the stretching vibration of the C-H bond in methyl and C=N stretching vibration in the imidazole ring, respectively. The peaks were at 3,430 cm^{-1} originated from a hydroxyl group in the form of physically adsorbed water. The stretching vibration in the imidazole ring was at 1,423 cm^{-1}. The non-planar vibration band was at 1,171–1,140 cm^{-1}, and the plane-bending vibration band was at 992 cm^{-1}. The results

TABLE 4 | Solid-state rate and integral expressions for different models.

Model	Differential form $f(\alpha) = 1/k.d\alpha/dt$	Integral form $g(\alpha) = kt$
Nucleation model		
Power law (P2)	$2\alpha^{1/2}$	$\alpha^{1/2}$
Power law (P3)	$3\alpha^{2/3}$	$\alpha^{1/3}$
Power law (P4)	$4\alpha^{3/4}$	$\alpha^{1/4}$
Avrami–Erofeyev (A2)	$2(1-\alpha)[-\ln(1-\alpha)]^{1/2}$	$[-\ln(1-\alpha)]^{1/2}$
Avrami–Erofeyev (A3)	$3(1-\alpha)[-\ln(1-\alpha)]^{2/3}$	$[-\ln(1-\alpha)]^{1/3}$
Avrami–Erofeyev (A4)	$4(1-\alpha)[-\ln(1-\alpha)]^{3/4}$	$[-\ln(1-\alpha)]^{1/4}$
Prout–Tompkins (B1)	$\alpha(1-\alpha)$	$\ln[\alpha/(1-\alpha)] + c^a$
Geometric control model		
Contracting area (R2)	$2(1-\alpha)^{1/2}$	$1-(1-\alpha)^{1/2}$
Contracting volume (R3)	$3(1-\alpha)^{2/3}$	$1-(1-\alpha)^{1/3}$
Diffusion model		
1D diffusion (D1)	$1/(2\alpha)$	α^2
2D diffusion (D2)	$-[1/\ln(1-\alpha)]$	$((1-\alpha)\ln(1-\alpha)) + \alpha$
3D diffusion–Jander (D3)	$[3(1-\alpha)^{2/3}]/[2(1-(1-\alpha)^{1/3})]$	$(1-(1-\alpha)^{1/3})^2$
Ginstling–Brounshtein (D4)	$3/[2((1-\alpha)^{-1/3}-1)]$	$1-(2/3)\alpha-(1-\alpha)^{2/3}$
Reaction series model		
Zero-order (F0/R)	1	α
First-order (F1)	$(1-\alpha)$	$[-\ln(1-\alpha)]$
Second-order (F2)	$(1-\alpha)^2$	$[1/(1-\alpha)]-1$
Third-order (F3)	$(1-\alpha)^3$	$(1/2)[(1-\alpha)^{-2}-1]$

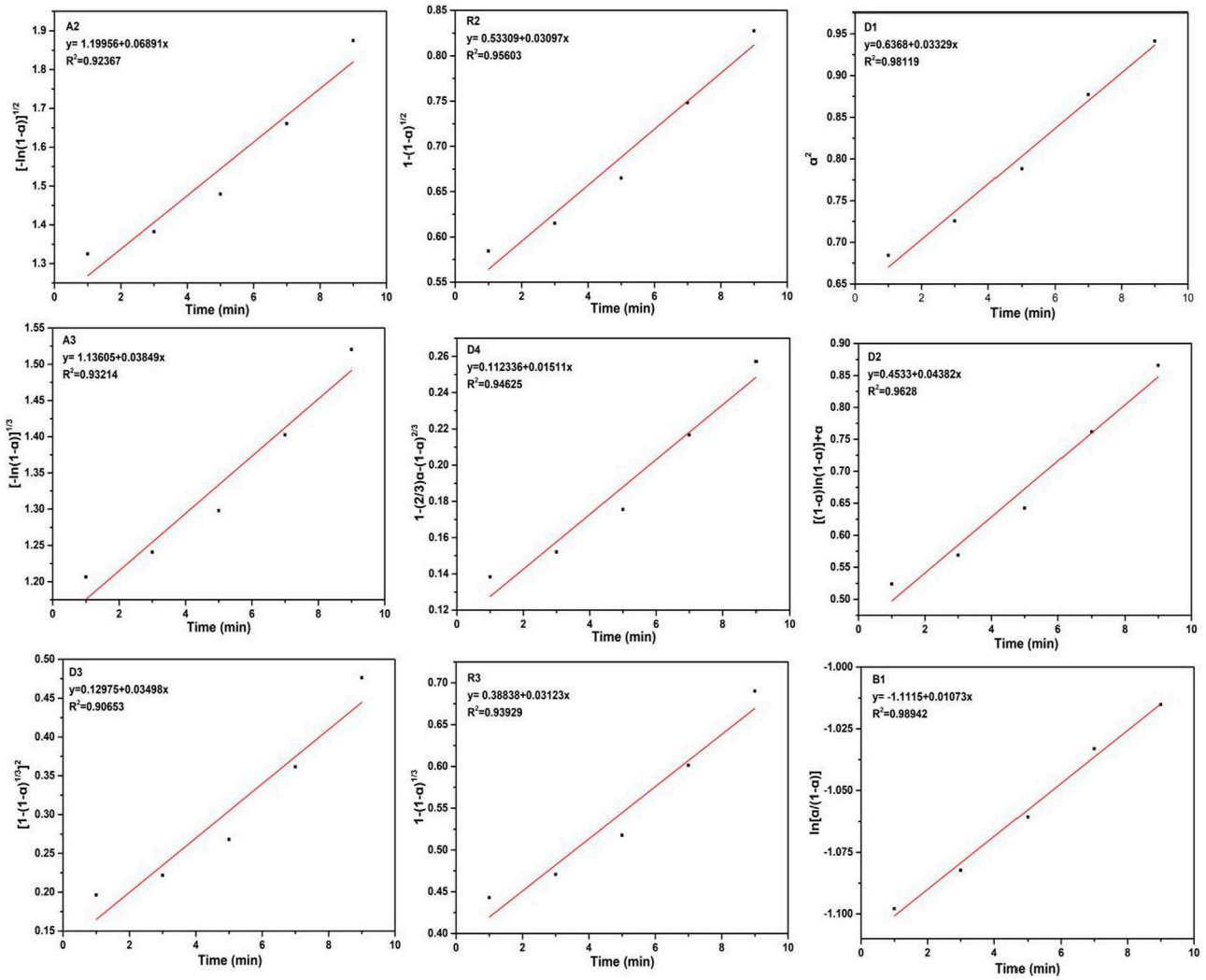

FIGURE 10 | Fitting of the I_t/I_{max} reaction of CoO with 2-methylimidazole after linearization to ten different models of solid-state reactivity of the A2 model; A3 model; D1 model; D2 model; D3 model; D4 model; R2 model; R3 model; and B1 model.

showed that ZIF-67 has been synthesized successfully (Qi et al., 2011).

From the P-XRD of ZIF-67, it could be found that the attribution of the diffraction peaks was in good agreement with the previous studies, as shown in **Figure 3**, and could be easily indexed as 7.31 (001), 10.36 (002), 12.66 (112), 14.62 (022), 16.38 (013), 17.92 (222), 22.15 (114), 24.53 (233), 25.62 (224), 26.70 (134), 29.67 (044), 30.62 (334), and 32.43 (235). This confirmed that ZIF-67 nanocrystals were well constructed (Chaudhary et al., 2013).

In order to observe the micro-surface morphology, the prepared ZIF-67 was analyzed by scanning electron microscopy (SEM). The surface of ZIF-67 is shown in **Figure 4**. It could be seen that the morphological characteristics of ZIF-67 was basically the same as reported in the literature (29–30). SEM revealed that the particles were nanocrystals with a polyhedral shape. The mean particle size was calculated as 50 nm. The obtained nanoparticles could be well dispersed in methanol and could be kept without settlement (Chaudhary et al., 2018; Mondal et al., 2019; Potbhare et al., 2019).

At the same time, we analyzed the prepared ZIF-67 using a transmission electron microscope (TEM) to observe its internal structure, as shown in **Figure 5**. We can see that the internal texture of ZIF-67 was solid and uniformly stacked, with good crystallinity. The morphology of ZIF-67 was consistent with that of SEM images, and it also showed the shape of near-dodecahedron. TEM analysis results showed that no agglomeration occurred between the ZIF-67 particles, and most of the particle sizes were also about 100 nm (Du et al., 2017).

ZIF-67 was dissolved in methanol, and the methanol solution was vaporized slowly at room temperature to yield the light purple crystals. The tested single crystal size was 0.13 × 0.12 × 0.11 mm. The data of ZIF-67 are summarized in **Table 1**. The

collected 3,465 diffraction points included independent 854 diffraction points (R_{int} = 0.0247). The structure was solved by direct methods with the SHELXS-97 program. The results showed that the formulas were $C_8H_{10}CoN_4$, the relative molecular weight was 221.13, and the density was 0.878 g cm^{-3}. $C_8H_{10}CoN_4$ crystallized in the cubic system I-43m space group. The unit lattice and crystal structure of ZIF-67 is shown in **Figure 6**.

Unlike ZIF-67 prepared by the solvent thermal method, comparing the cell-stacking patterns of two kinds of ZIF-67 single crystals, it was easy to find that there was no crystal water or coordination water in unit lattice of ZIF-67 prepared by AFI, which was because we did not introduce solvents in the synthesis process. Selected bond lengths and angles of ZIF-67 are presented in **Tables 2**, **3**.

Thermal Stability

In order to further verify the thermal performance of ZIF-67, we used DTA and TG to analyze the thermal properties.

The DTA was heated from room temperature to 600°C with a heating rate of 10°C min^{-1} under air. As shown in **Figure 7**, the decomposition peak temperature of ZIF-67 was 371°C, with a sharp peak shape and high-heat release, and showed good thermal stability.

In **Figure 8**, TG also proved the thermal stability; ZIF-67 had no weight loss before 300°C. In the first stage, the material lost about 47%, which was due to the decomposition of organic ligands, and the weight loss process ended at 520°C. It showed that the ZIF-67 material can be stabilized at 350°C (Kim et al., 2010; Friščić et al., 2013; Mottillo et al., 2013).

Kinetic Analysis

Therefore, an *ex situ* P-XRD technique was used for studying the mechanisms and kinetics of the AFI preparation process. Compared with other monitoring techniques, P-XRD had the advantages of simple operation, low-testing cost, and good reproducibility.

For another, owing to the different phase composition of CoO, 2-methylimidazole, and ZIF-67, these compounds had different characteristic diffraction peaks. We found a new diffraction peak appeared at 7.3°, contributing to the characteristic diffraction peak of ZIF-67; the characteristic diffraction peak became stronger with the increase of reaction time. P-XRD tests at different times are shown in **Figure 9**. The integral expressions are in **Table 4**, and the fitting results are shown in **Figure 10** (Banerjee et al., 2008; Wang et al., 2008; Chen et al., 2019).

For ZIF-67, the experimental data were most consistent with the 1D kinetic model, indicating that the mechanism of ZIF-67 belonged to the one-dimensional diffusion-controlled model. The R^2 of the fitting result reached 0.98119.

The mixed materials of cobalt oxide and 2-methylimidazole obtained high kinetic energy through the accelerating nozzle, and friction and collision continued to occur between the raw materials. 2-Methylimidazole first attaches to the surface of cobalt oxide and then collides with the target. The kinetic energy overcame the reaction activation energy, resulting in lattice defects of molecules, and then the covalent bonds between molecules break and produce new coordination bonds.

CONCLUSION

In summary, the ZIF-67 was successfully prepared by AFI, and its single crystal was obtained by methanol evaporation. Also, the ZIF-67 was characterized by FT-IR, P-XRD, DTA/TG, and single-crystal x-ray diffraction. All of the results indicated that the ZIF-67 was successfully synthesized at a rate of 60 kg h^{-1}. The mechanisms of ZIF-67 reactions have been investigated, and the kinetic data suggested that the mechanisms were consistent with 1D models. We demonstrated that AFI can be a novel and effective technique for the mechanochemical synthesis of MOFs under solvent-free conditions.

DATA AVAILABILITY STATEMENT

The datasets presented in this study can be found in online repositories. The names of the repository/repositories and accession number(s) can be found below: https://ccdc.cam.ac.uk/ CCDC-1945392.

AUTHOR CONTRIBUTIONS

The author confirms being the sole contributor of this work and has approved it for publication.

FUNDING

This work was supported by the Major Frontier Innovation Project of Science and Technology Department of Sichuan Province (project no.: 2019YJ0447), Sichuan Provincial Science and Technology Department's Major Frontier Project of Applied Basic Research (2019YJ0447), Project of State Key Laboratory of Environment-friendly Energy Materials, Southwest University of Science and Technology (19fksy04), and National Natural Science Foundation of China (project no.: 51972278).

REFERENCES

Baláž, P., Achimovičová, M., Baláž, M., Billik, P., Zheleva, Z. C., Criado, J. M., et al. (2013). Hallmarks of Mechanochemistry: from Nanoparticles to Technology. *Chem. Soc. Rev.* 42 (18), 7571–7637. doi:10.1039/c3cs35468g

Banerjee, R., Phan, A., Wang, B., Knobler, C., Furukawa, H., O'Keeffe, M., et al. (2008). High-Throughput Synthesis of Zeolitic Imidazolate Frameworks and Application to CO 2 Capture. *Science* 319, 939–943. doi:10.1126/science.1152516

Bennett, T. D., Saines, P. J., Keen, D. A., Tan, J.-C., and Cheetham, A. K. (2013). Ball-Milling-Induced Amorphization of Zeolitic Imidazolate Frameworks

(ZIFs) for the Irreversible Trapping of Iodine. *Chem. Eur. J.* 19 (22), 7049–7055. doi:10.1002/chem.201300216

Chaudhary, R. G., Sonkusare, V. N., Bhusari, G. S., Mondal, A., Shaik, D., and Juneja, H. D. (2018). Microwave-mediated Synthesis of Spinel $CuAl_2O_4$ Nanocomposites for Enhanced Electrochemical and Catalytic Performance [J]. *Res. Chem. Intermediates* 44, 2039–2060. doi:10.1007/s11164-017-3213-z

Chaudhary, R. G., Juneja, H. D., and Gharpure, M. P. (2013). Thermal Degradation Behaviour of Some Metal Chelate Polymer Compounds with Bis(bidentate) Ligand by TG/DTG/DTA. *J. Therm. Anal. Calorim.* 112, 637–647. doi:10.1007/s10973-012-2616-8

Chen, D., Zhao, J., Zhang, P., and Dai, S. (2019). Mechanochemical Synthesis of Metal-Organic Frameworks. *Polyhedron* 162, 59–64. doi:10.1016/j.poly.2019.01.024

Crawford, D., Casaban, J., Haydon, R., Giri, N., McNally, T., and James, S. L. (2015). Synthesis by Extrusion: Continuous, Large-Scale Preparation of MOFs Using Little or No Solvent. *Chem. Sci.* 6 (3), 1645–1649. doi:10.1039/c4sc03217a

Crawford, D. E., and Casaban, J. (2016). Recent Developments in Mechanochemical Materials Synthesis by Extrusion. *Adv. Mater.* 28 (27), 5747–5754. doi:10.1002/adma.201505352

Du, X.-D., Wang, C.-C., Liu, J.-G., Zhao, X.-D., Zhong, J., Li, Y.-X., et al. (2017). Extensive and Selective Adsorption of ZIF-67 towards Organic Dyes: Performance and Mechanism. *J. Colloid Interf. Sci.* 506, 437–441. doi:10.1016/j.jcis.2017.07.073

Friščić, T., Halasz, I., Beldon, P. J., Belenguer, A. M., Adams, F., Kimber, S. A., et al. (2013). Real-time and *In Situ* Monitoring of Mechanochemical Milling Reactions. *Nat. Chem.* 5, 66–73. doi:10.1038/nchem.1505

James, S. L., Adams, C. J., Bolm, C., Braga, D., Collier, P., Friščić, T., et al. (2012). Mechanochemistry: Opportunities for New and Cleaner Synthesis. *Chem. Soc. Rev.* 41 (1), 413–447. doi:10.1039/c1cs15171a

Kim, B. H., Hong, W. G., Lee, S. M., Yun, Y. J., Yu, H. Y., Oh, S.-Y., et al. (2010). Enhancement of Hydrogen Storage Capacity in Polyaniline-Vanadium Pentoxide Nanocomposites. *Int. J. Hydrogen Energ.* 35, 1300–1304. doi:10.1016/j.ijhydene.2009.11.089

Mondal, A., Giri, N., Sarkar, S., Majumdar, S., and Ray, R. (2019). Tuning the Photocatalytic Activity of ZnO by TM (TM = Fe, Co, Ni) Doping. *Mater. Sci. Semiconductor Process.* 91, 333–340. doi:10.1016/j.mssp.2018.12.003

Mottillo, C., Lu, Y., Pham, M.-H., Cliffe, M. J., Do, T.-O., and Friščić, T. (2013). Mineral Neogenesis as an Inspiration for Mild, Solvent-free Synthesis of Bulk Microporous Metal-Organic Frameworks from Metal (Zn, Co) Oxides. *Green. Chem.* 15, 2121–2131. doi:10.1039/c3gc40520f

Panda, T., Horike, S., Hagi, K., Ogiwara, N., Kadota, K., Itakura, T., et al. (2017). Mechanical Alloying of Metal-Organic Frameworks. *Angew. Chem.* 129 (9), 2453–2457. doi:10.1002/ange.201612587

Potbhare, A. K., Chaudhary, R. G., Chouke, P. B., Yerpude, S., Mondal, A., Sonkusare, V. N., et al. (2019). Phytosynthesis of Nearly Monodisperse CuO Nanospheres Using Phyllanthus Reticulatus/Conyza Bonariensis and its Antioxidant/antibacterial Assays. *Mater. Sci. Eng. C* 99, 783–793. doi:10.1016/j.msec.2019.02.010

Qi, S., Chen, Z., Song, Z., Li, J., and Dong, J. (2011). Synthesis of ZIF-8 and ZIF-67 by Steam-Assisted Conversion and an Investigation of Their Tribological Behaviors. *Angew. Chem. Int. Ed. Engl.* 50, 672–675. doi:10.1002/anie.201004937

Qian, J., Sun, F., and Qin, L. (2012). Hydrothermal Synthesis of Zeolitic Imidazolate Framework-67 (ZIF-67) Nanocrystals. *Mater. Lett.* 82, 220–223. doi:10.1016/j.matlet.2012.05.077

Qin, J., Wang, S., and Wang, X. (2017). Visible-light Reduction CO 2 with Dodecahedral Zeolitic Imidazolate Framework ZIF-67 as an Efficient Co-catalyst. *Appl. Catal. B: Environ.* 209, 476–482. doi:10.1016/j.apcatb.2017.03.018

Stock, N., and Biswas, S. (2012). Synthesis of Metal-Organic Frameworks (MOFs): Routes to Various MOF Topologies, Morphologies, and Composites. *Chem. Rev.* 112, 933–969. doi:10.1021/cr200304e

Sun, B., He, Y., Peng, R., Chu, S., and Zuo, J. (2016). Air-flow Impacting for Continuous, Highly Efficient, Large-Scale Mechanochemical Synthesis: a Proof-Of-Concept Study. *ACS Sustainable Chem. Eng.* 4, 2122–2128. doi:10.1021/acssuschemeng.5b01579

Takacs, L. (2013). The Historical Development of Mechanochemistry. *Chem. Soc. Rev.* 42 (18), 7649–7659. doi:10.1039/c2cs35442j

Wang, B., Côté, A. P., Furukawa, H., O'Keeffe, M., and Yaghi, O. M. (2008). Colossal Cages in Zeolitic Imidazolate Frameworks as Selective Carbon Dioxide Reservoirs. *Nature* 453, 207–211. doi:10.1038/nature06900

Wang, G.-W. (2013). Mechanochemical Organic Synthesis. *Chem. Soc. Rev.* 42 (18), 7668–7700. doi:10.1039/c3cs35526h

Wang, M., Liu, J., Guo, C., Gao, X., Gong, C., Wang, Y., et al. (2018). Metal-organic Frameworks (ZIF-67) as Efficient Cocatalysts for Photocatalytic Reduction of CO2: the Role of the Morphology Effect. *J. Mater. Chem. A.* 6, 4768–4775. doi:10.1039/c8ta00154e

Zheng, J., Cui, X., Yang, Q., Ren, Q., Yang, Y., and Xing, H. (2018). Shaping of Ultrahigh-Loading MOF Pellet with a Strongly Anti-tearing Binder for Gas Separation and Storage. *Chem. Eng. J.* 354, 1075–1082. doi:10.1016/j.cej.2018.08.119

Zhou, S., Ye, Z., Hu, S., Hao, C., Wang, X., Huang, C., et al. (2018). Designed Formation of Co3O4/ZnCo2O4/CuO Hollow Polyhedral Nanocages Derived from Zeolitic Imidazolate Framework-67 for High-Performance Supercapacitors. *Nanoscale* 10, 15771–15781. doi:10.1039/c8nr05138k

Conflict of Interest: The author declares that the research was conducted in the absence of any commercial or financial relationships that could be construed as a potential conflict of interest.

Publisher's Note: All claims expressed in this article are solely those of the authors and do not necessarily represent those of their affiliated organizations, or those of the publisher, the editors, and the reviewers. Any product that may be evaluated in this article, or claim that may be made by its manufacturer, is not guaranteed or endorsed by the publisher.